A two-phase model based on unified formulation for continuum mechanics applied to sediment transport in geophysical flows: Application to sedimentation, consolidation and erosion. Study case- the Gironde Estuary (France)

K.D. Nguyen

Laboratory Saint-Venant for Hydraulics, Université PARIS-EST, 78400 CHATOU , FRANCE

Thanks to my co-workers

- Sylvain Guillou(1993-present)- University of Caen
- Damien Pham-Van-Bang (2008-present), Lab Saint-Venant, Université Paris-Est
- Nataly Barbry (Ph.D., 1996-2000, University of Caen)
- Julien Chauchat (Ph.D., 2003-2007, Post-Doc, 2008 in University of Caen)
- Duc Hau Nguyen (Ph.D. 2008-2011, University of Caen)
- Miguel Uh-Zapata, Post-Doc, 2011-present)
- Shafuil Islam (Ph.D., 2012-present, Université Paris-Est)

CONTEXT

- Requirement from a lot of applications of sediment transport modelling: Turbidity maximum in estuaries, Dredging operation, silting and scouring process, ...
- Scientific Challenges:
  - Physical challenges: Rheology of sediments, very dense flows, fluid-bed interaction, liquid-like and solid-like of solid fraction, and turbulence ..
  - Numerical challenges & parallelisation (MPI-CPU, CUDA-GPU)

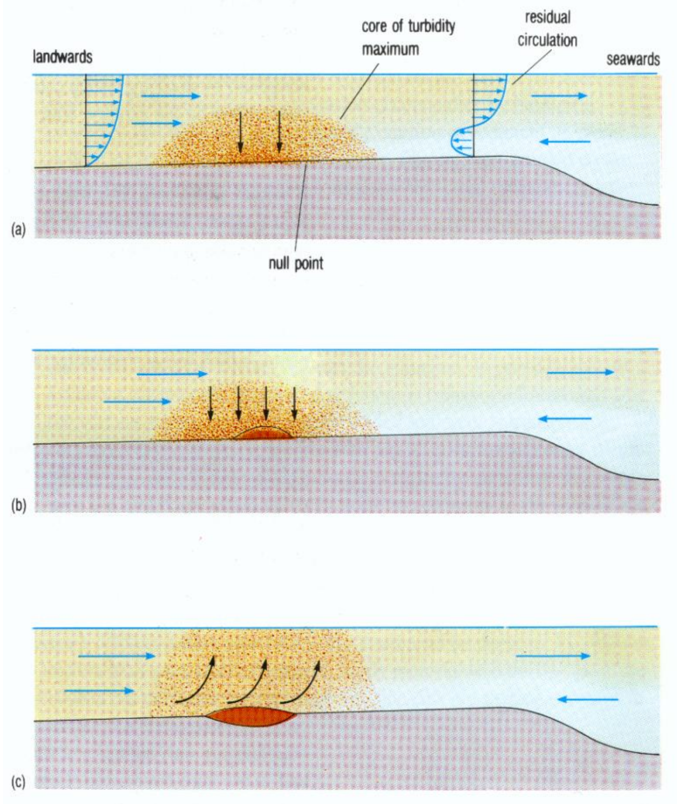

FORMATION OF TURBIDITY MAXIMUM IN ESTUARIES

PROCESSING OF SEDIMENT TRANSPORT

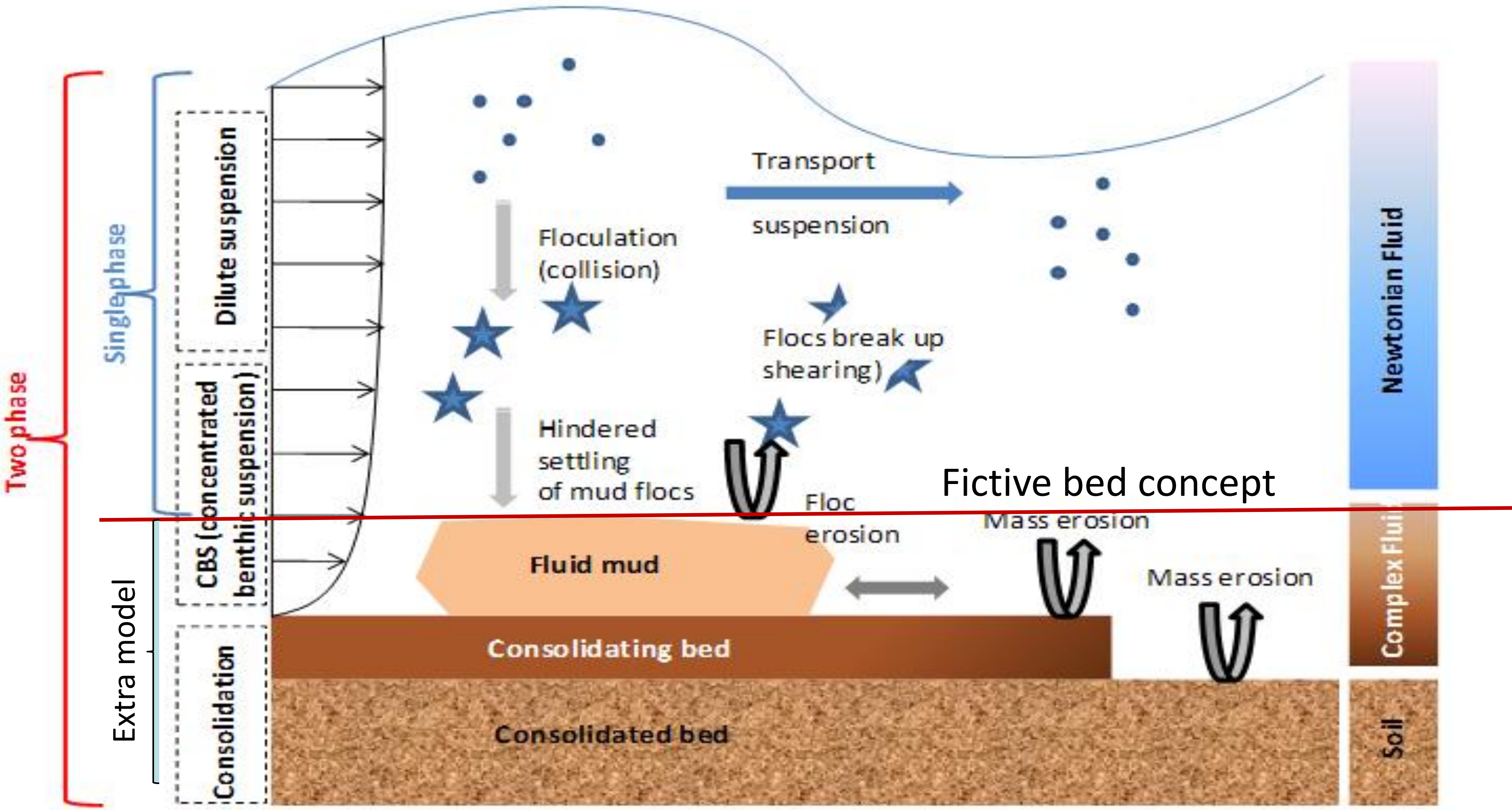

CONTENTS

REMARKS ON SINGLE- AND TWO-PHASE MODEL

Single-phase Models

- "Passive scalar" hypothesis
- No fluid-particles interactions. Fluid-bed interaction by empiric formulas for deposit and erosion fluxes
- Fictive-bed conception
- Extra models for consolidation of solid particles

Unphysical description for very dense flows (?) -Small computing cost
Acceptable to engineering problems

Two-phase Models

- No "passive scalar" hypothesis
- Fluid-particles interaction. Fluid-bed interaction by the models
- No fictive-bed conception
- Consolidation process included in the models

All interactions considered
Correct physical description
High computing cost

OBJECTIVES of THIS WORK

- To develop a two-phase model that is able to simulate the main processes of sediment transport in estuarine and coastal zones, such as suspension, sedimentation, consolidation and erosion. (*The computing domain should cover from non-erodible beds to free water surfaces*).
- To propose efficient CFD and HPC techniques, which provide the high accuracy and the reduction of computing cost.

DESCRIPTION FOR TWO-PHASE MODEL

- Two-phase (fluid & solid particles) model with unified formulation for continuum mechanics (Navier-Stokes and Navier Equations)
- Non hydrostatic pressure
- k-ε turbulence model (K_f, ε_f, K_s and K_{sf}) , K-Ω and LES (in progress)
- Adaptative Eulerian mesh in Z and unstructured in (x,y)
- Projection method + Finite volume method
- 2-D Vertical Version completed (parallelised by MPI-CPU, CUDA-GPU)
- 3-D version development in progress (Summer 2014)

- Averaged equations

$$\frac{\partial(\alpha_k \rho_k B)}{\partial t} + \vec{\nabla}.(\alpha_k \rho_k \vec{u}_k B) = 0$$

$$\frac{\partial(\alpha_k \rho_k \vec{u}_k)}{\partial t} + \vec{\nabla}.(\alpha_k \rho_k \vec{u}_k \otimes \vec{u}_k) = \vec{\nabla}.\left(-\alpha_k p_k \overline{\overline{I}} + \alpha_k \overline{\overline{\tau_k}}\right) + \alpha_k \rho_k \vec{g} + \vec{M}_k$$

Effective Stress for solid phase

$$p_s = \tilde{p} + \sigma_e \quad \text{with} \quad \sigma_e = 50\left(\frac{\alpha_s - \alpha_s^{gel}}{\alpha_s^{\max} - \alpha_s}\right) \quad \textit{For} \quad \alpha_s > \alpha_{gel}$$

- Closure Laws

Transfer laws

$$\vec{M}_k = p_{ki}\vec{\nabla}\alpha_k - \vec{\vec{\tau}}_{ki}\vec{\nabla}\alpha_k + \vec{M}'_k$$

$$p_{si} = p_{fi} + H\sigma_{pi}$$

$$p_{fi} = p_f - \frac{1}{4}\rho_f\left|\vec{u}_f - \vec{u}_s\right|^2$$

$$\vec{\vec{\tau}}_{si} = \vec{\vec{\tau}}_{fi} = \beta\ \vec{\vec{\tau}}_f$$

$$\vec{\vec{\tau}}_f = \mu_f\ (\vec{\nabla}\ \vec{u}_f + (\vec{\nabla}\ \vec{u}_f)^T)$$

$$\vec{M}'_s = \vec{F}_D + \vec{F}_{vm} + \vec{F}_L + \vec{F}_F + \vec{F}_B$$

$$\vec{M}'_f = -\vec{M}'_s$$

Constitutive laws

Viscous Stresses

$$\vec{\nabla}.\left(\alpha_f \overline{\overline{\tau_f}}\right)=\frac{1}{B}\left[\vec{\nabla}.\left(\mu_{ff}\overline{\overline{D_f}}\right)+\vec{\nabla}.\left(\mu_{fs}\overline{\overline{D_s}}\right)\right]$$

$$\vec{\nabla}.\left(\alpha_s \overline{\overline{\tau_s}}\right)=\frac{1}{B}\left[\vec{\nabla}.\left(\mu_{sf}\overline{\overline{D_f}}\right)+\vec{\nabla}.\left(\mu_{ss}\overline{\overline{D_s}}\right)\right]$$

$$\overline{\overline{D_k}}=\frac{1}{2}\left[\vec{\nabla}\otimes(\vec{u}_k B)+\left(\vec{\nabla}\otimes(\vec{u}_k B)\right)^T\right]$$

$$\beta=\frac{5}{2}+\frac{9}{4}\left[\frac{1}{1+h/d}\right]\left[\frac{1}{(2h/d)}-\frac{1}{(1+2h/d)}-\frac{1}{(1+2h/d)^2}\right]\frac{1}{\alpha_s}$$

$$\mu_{ff}=\alpha_f\mu_f \qquad \mu_{ss}=\alpha_s{}^2\beta\mu_f$$

$$\mu_{fs}=\alpha_s\mu_f \qquad \mu_{sf}=\alpha_s\alpha_f\beta\mu_f$$

$$\mu_{f\nabla}=-\mu_f \qquad \mu_{s\nabla}=\alpha_s\beta\mu_{f\nabla}$$

Particles Pressure

$$\vec{\nabla}(\alpha_s p_s)=\vec{\nabla}(\alpha_s p_{s,cin})+\vec{\nabla}(\alpha_s p_{s,coll})+\vec{\nabla}(\alpha_s p_f)$$

$$\vec{\nabla}(\alpha_s p_{s,coll})=-G(\alpha_f)\,\vec{\nabla}\alpha_s$$

$$G(\alpha_f)=10^{B_1\alpha_f+B_2}$$

$$G(\alpha_f)=G_0 e^{-C(\alpha_f-\alpha^*)}$$

CFD Techniques: Advection terms

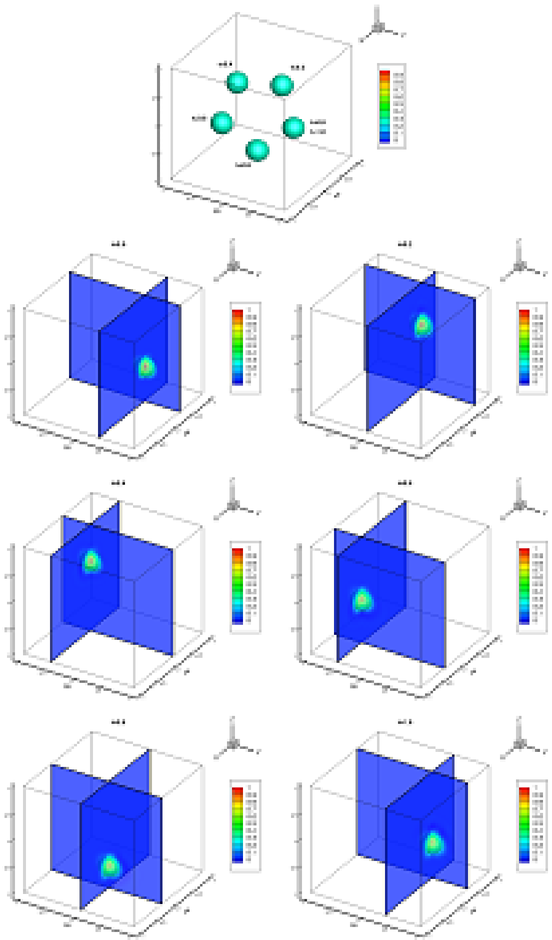

Figure 1.8: Solution of the three-dimensional advection problem with a solid-body rotation flow field as velocity field at times $t = 0.0, 0.2, 0.4, 0.6, 0.8, 1.0$ for $N = 64$.

Advection equation

$$\frac{\partial(\alpha_k \rho_k u_k)}{\partial t} + \nabla.(\alpha_k \rho_k u_k u_k) = 0 \rightarrow \frac{\partial \emptyset}{\partial t} + \nabla.(\emptyset\, u) = 0$$

Numerical Scheme: ULSS+LED (Nguyen et al., C&F, 2013)
Test-case:
The computational domain is [-1; 1] x [-1; 1]x[-1; 1]
The initial condition is an sphere of radius 0.25 with
The velocity field is a solid-body rotation flow field

N	Peak values	Maximun Absolute	Order
16	0.121	0.635	-
32	0.414	0.559	0.813
64	0.844	0.142	1.987
128	0.979	0.017	3.052

Table 1.2: Errors, peak values and numerical orders of accuracy of the three-dimensional advection problem after one full revolution at the time $t = 1.0$.

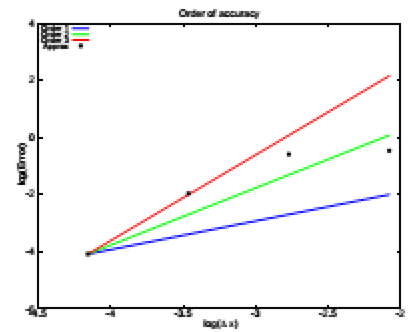

Figure 1.9: Convergence analysis for the three-dimensional advection problem after one full revolution. The $*$-marks denotes the results from the approximation, and the lines represent the ideal order of accuracy.

CFD Techniques: Poisson Equation

Poisson equation:

$$\frac{\partial}{\partial x}\left(\alpha_k \frac{\partial \delta p_k}{\partial x}\right)+\frac{\partial}{\partial y}\left(\alpha_k \frac{\partial \delta p_k}{\partial y}\right)+\frac{\partial}{\partial z}\left(\alpha_k \frac{\partial \delta p_k}{\partial z}\right) = \frac{\rho_k}{\Delta t}\left[-\frac{\partial \alpha_k}{\partial t} + \nabla \cdot (\alpha_k \mathbf{u}_k^*)\right]$$

where $\delta p = p^{n+1} - p^n$.

$$x^* = x, \quad y^* = y, \quad \sigma = \frac{z+h}{\eta+h}, \quad t^* = t$$

where η is the water surface level and h is the bottom depth.

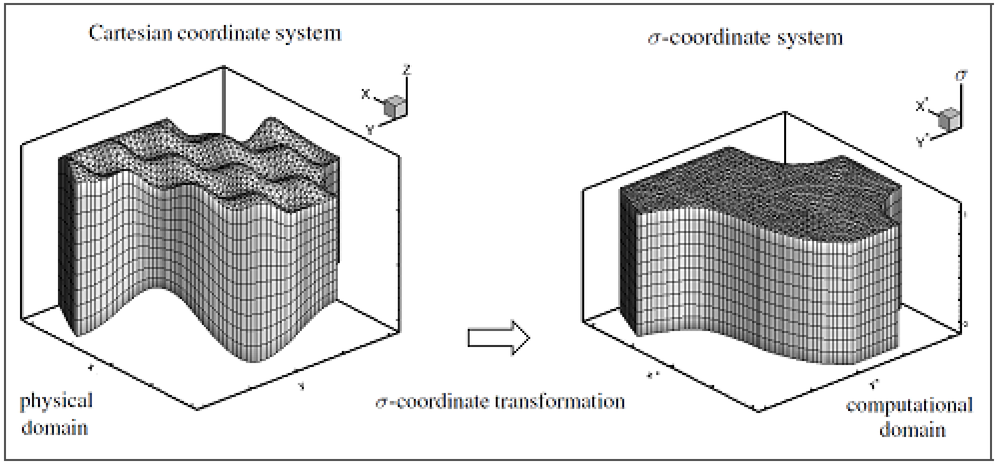

CFD Techniques: Poisson Equation (2/3)

- The Poisson equation is approximated given a right-hand side profile and compared with its corresponding analytical solution using $\Gamma = 1$.

  Right-hand side profile : $f(x, y) = 3\pi^2 \sin(\pi x) \sin(\pi y) \sin(\pi \sigma)$

  Analytical solution : $\phi(x, y) = \sin(\pi x) \sin(\pi y) \sin(\pi \sigma)$

- The first example has been solved over a box domain $[-1, 1] \times [-1, 1] \times [-1, 1]$ using three different types of grid:

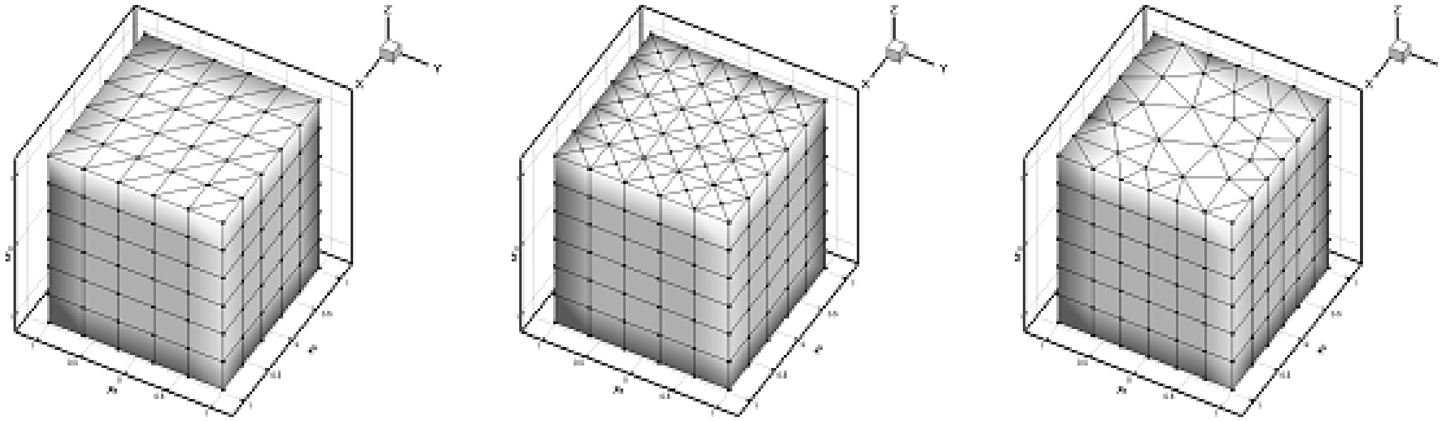

CFD Techniques: Poisson Equation (3/3)

Errors & Accuracy

Exact solution, approximation and errors using the grid type 2:

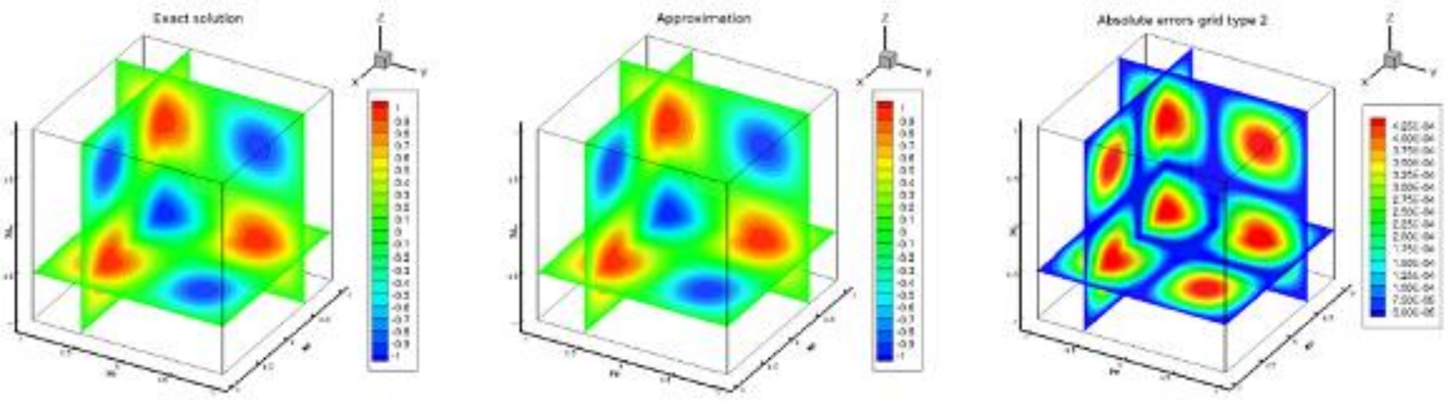

Maximum absolute errors and order of accuracy:

N	Grid type 1	Order	Grid type 2	Order	Grid type 3	Order
16	0.18×10^{-1}	-	0.80×10^{-2}	-	0.19×10^{-1}	-
32	0.44×10^{-2}	2.03	0.19×10^{-2}	2.08	0.56×10^{-2}	1.78
64	0.10×10^{-2}	2.03	0.46×10^{-3}	2.06	0.11×10^{-2}	2.05
128	0.26×10^{-3}	2.03	0.11×10^{-3}	2.02	0.28×10^{-3}	2.03

Sedimentation and Consolidation

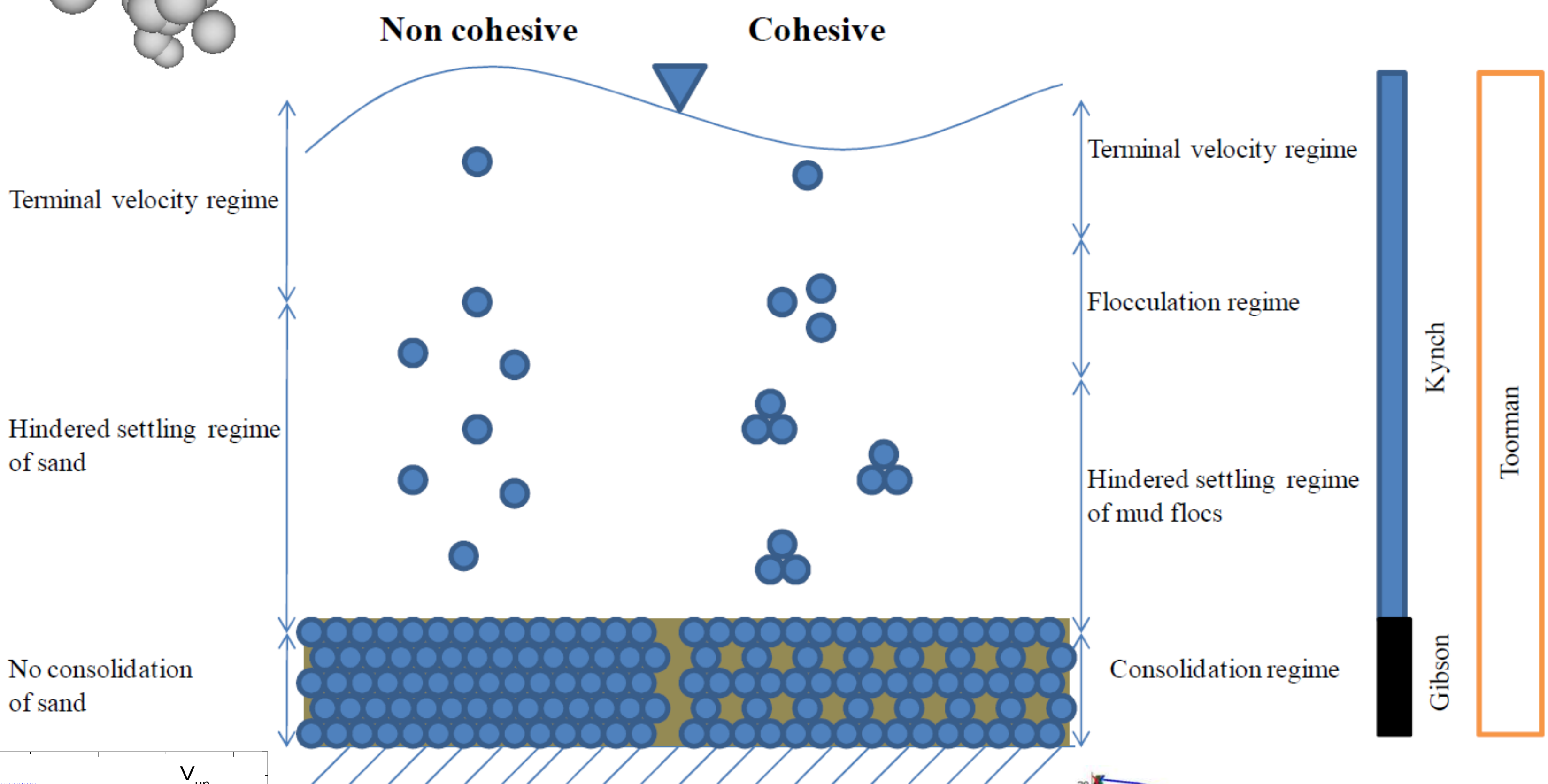

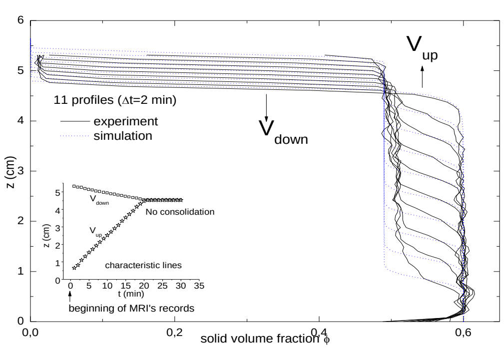

Sedimentation of granular (cohesionless) suspension by MRI
Pham Van Bang et al. 2008

Settling column tests on cohesive suspension (Gironde mud)
Villaret et al. 2010

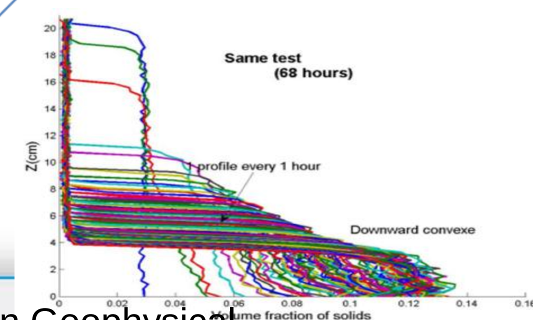

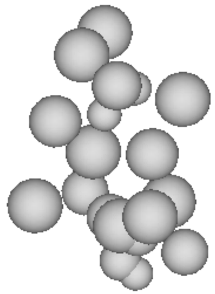

Sedimentation and Consolidation of non-cohesive particles

(Nguyen et al., Advances in Water Res., 2009, p 1187-1196)

Expérience réalisée au LMSGC [Pham Van Bang et al., 2006]

- Particules : billes de polystyrène
  - $D_p = 290 \pm 30\ \mu m$
  - $\rho_s = 1{,}05\ kg.m^{-3}$
  - α_s=0,48
- Fluide : huile de silicone
  - $\mu_f = 20.10^{-3} kg.m^{-1}.s^{-1}$
  - $\rho_f = 0{,}95\ kg.m^{-3}$

Paramètres numériques

- Maillage : 11 x 91
- $\Delta t = 5.10^{-4}$ s

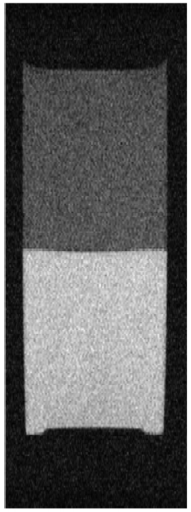

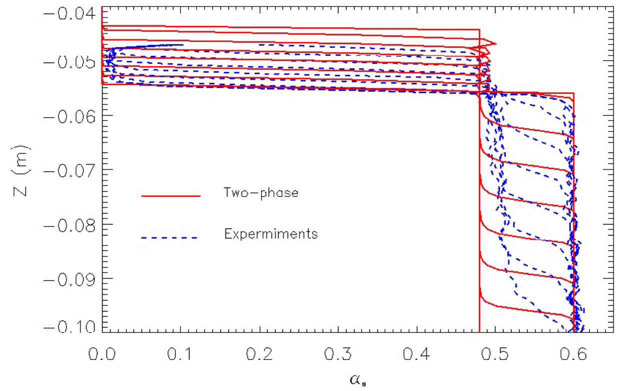

Profile de volume fraction of the solid phase

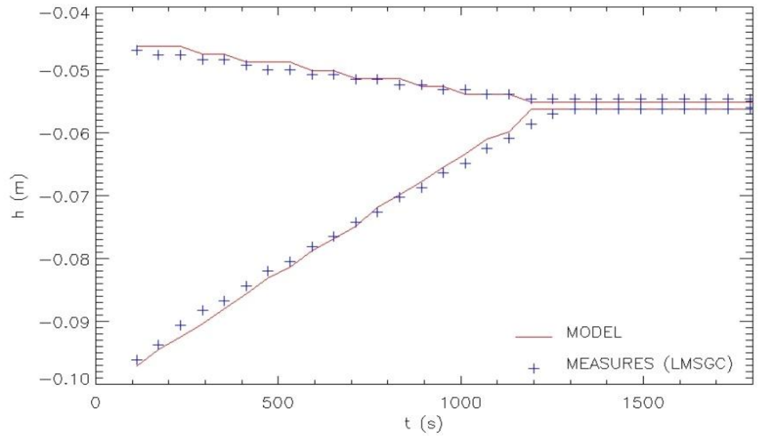

Evolution of the water-sediment interface

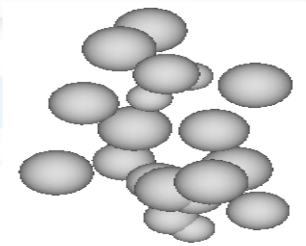

Sedimentation and Consolidation of cohesive particles (Kaolin)

(Chauchat et al., JHR, 2003, 2013.768798)

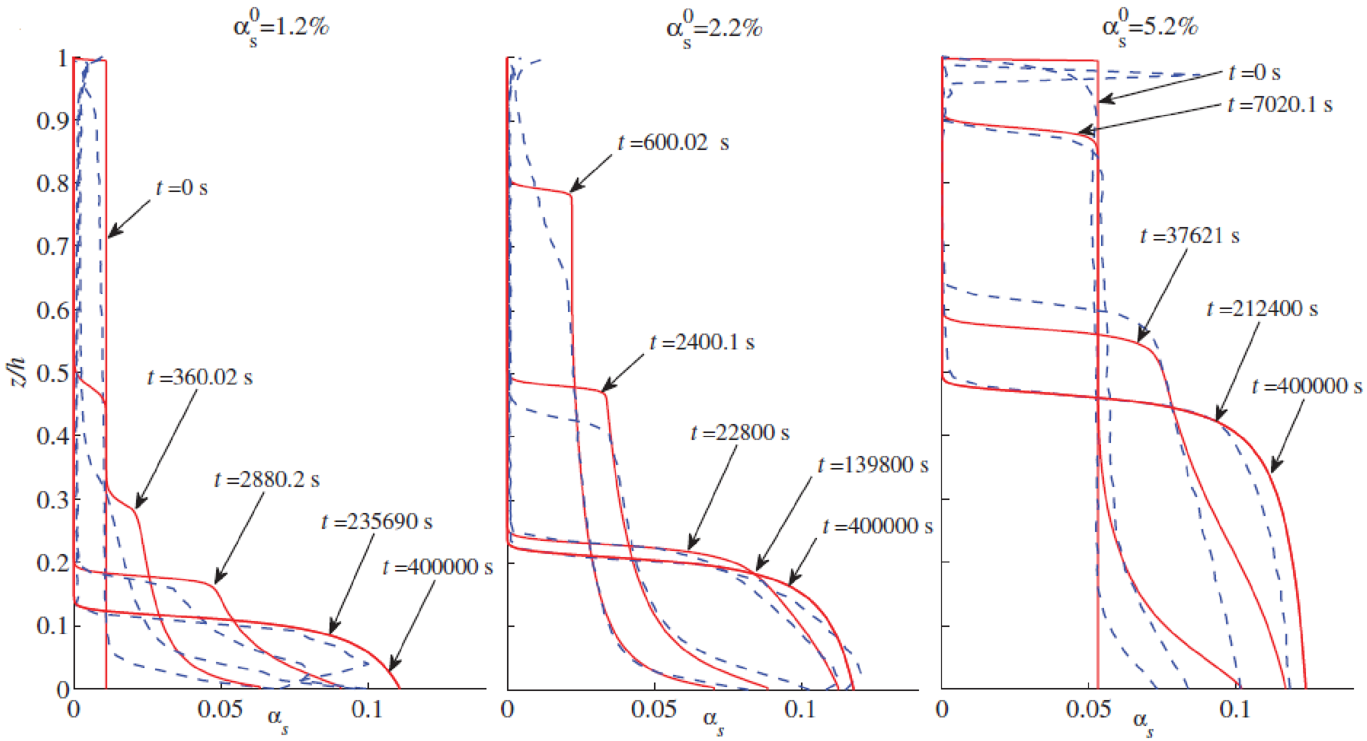

Comparison of two-phase model results with experiments for initial concentrations α*s* = 1.2, 2.2 and 5.2%. ime evolution of the mud–clear water interface position (symbols: experiments; lines: model) and (b) solid volume fraction profiles (dashed blue lines :experiments; solid red lines: model)

Dredged Sediment Release in Open Sea

(Nguyen et al., Advances in Water Res., 2012)

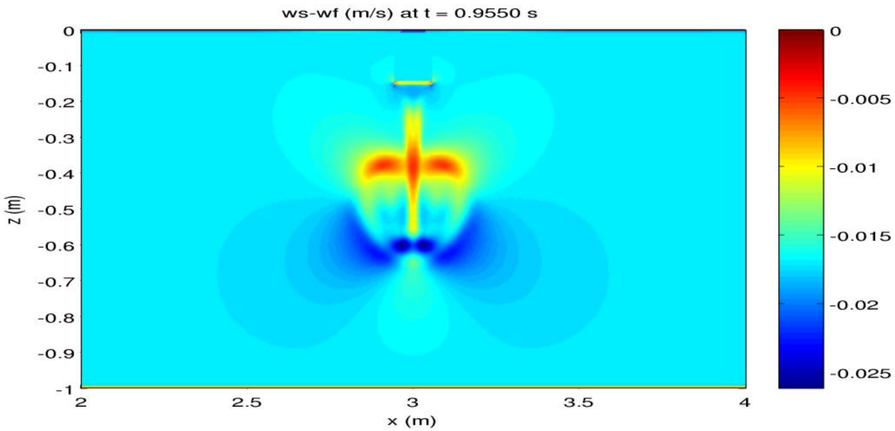

Isocontour map of the vertical-velocity lag between the fluid and solid phases (w_s-w_f= -w_{sett}).

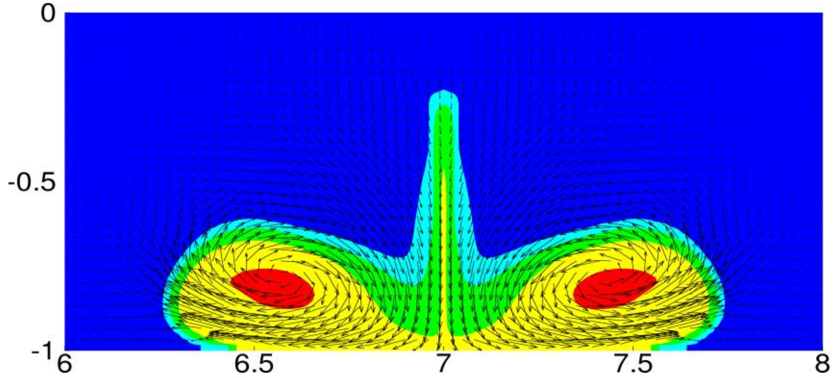

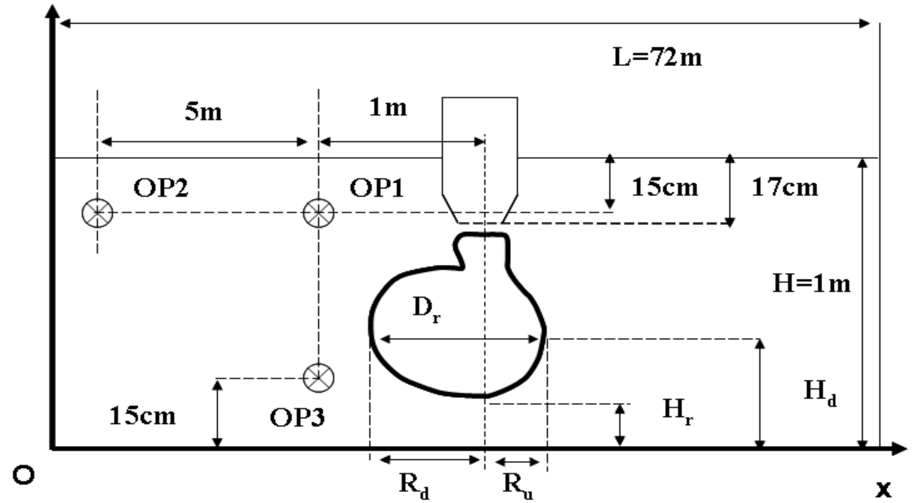

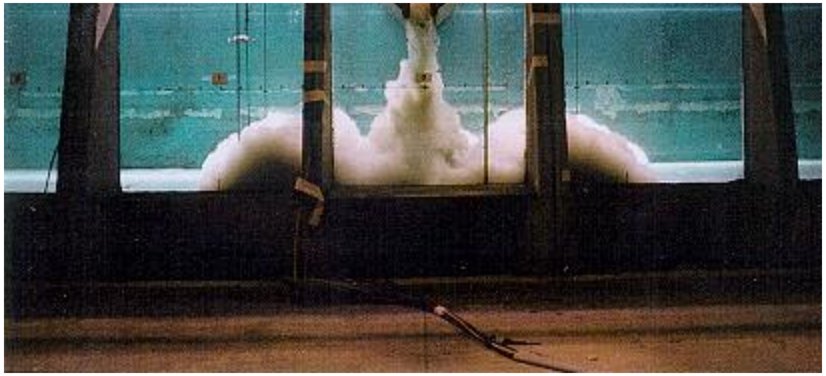

Fig. 1: Definition sketch: (upper) location of Optical Probes (OP) for turbidity measurements; (lower) sediment release (Boutin, 2000).

Comparison between single- and two-phase models
Case of sediment release in open sea

Single-phase

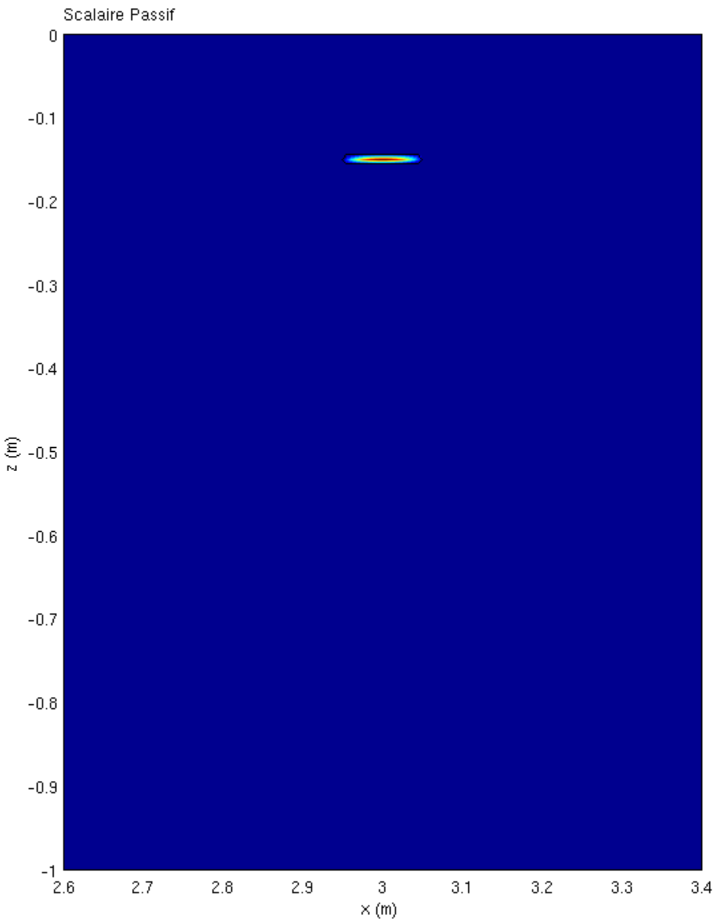

Two-phase

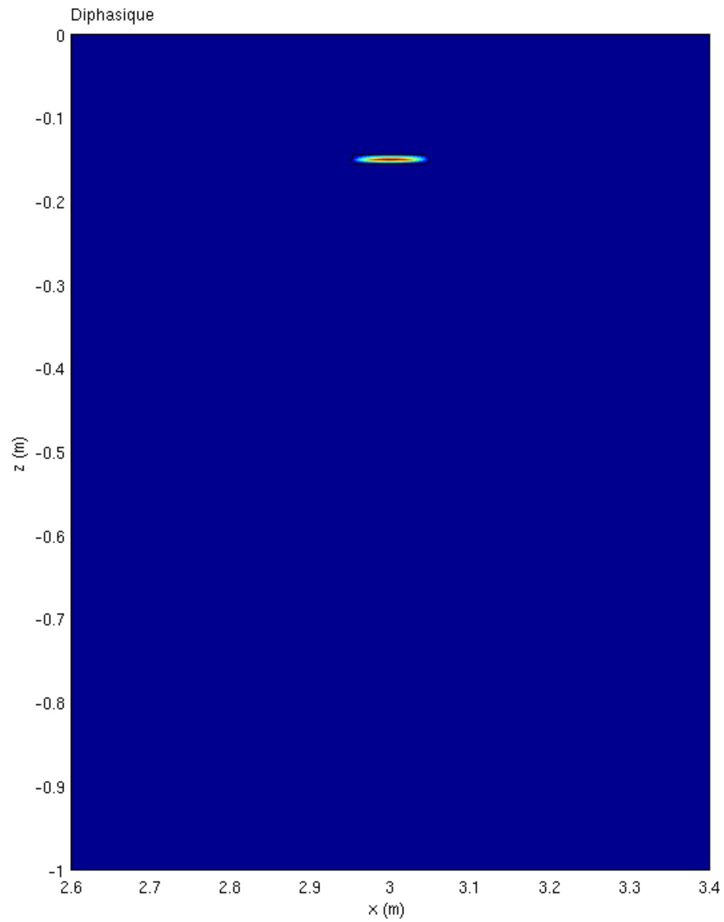

Dredged sediment release in open sea

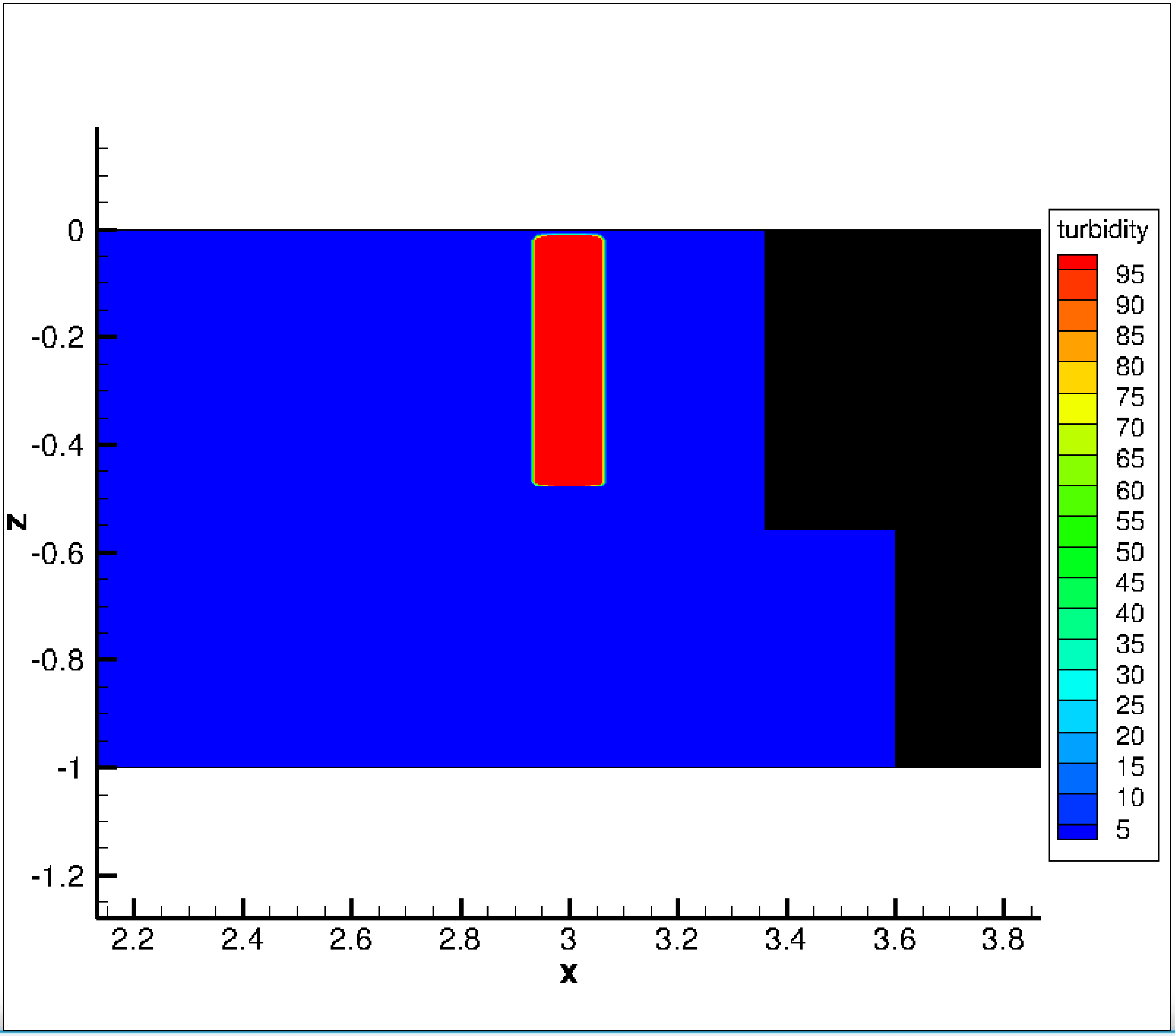

Water-Sediment Interface: Kelvin-Helmholtz Instability (1/3)

Non-cohesive | cohesive

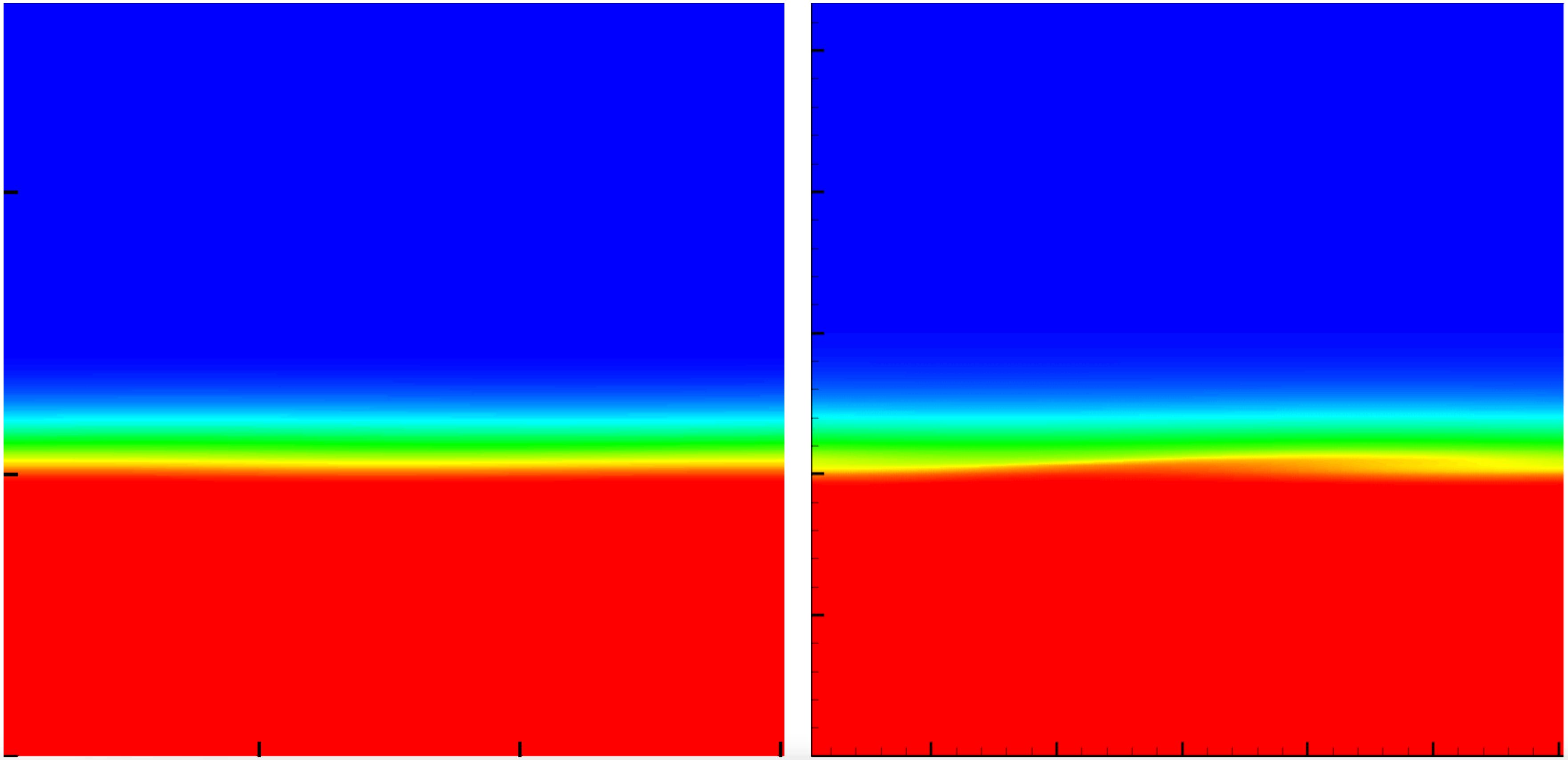

Étude de sensibilité au maillage

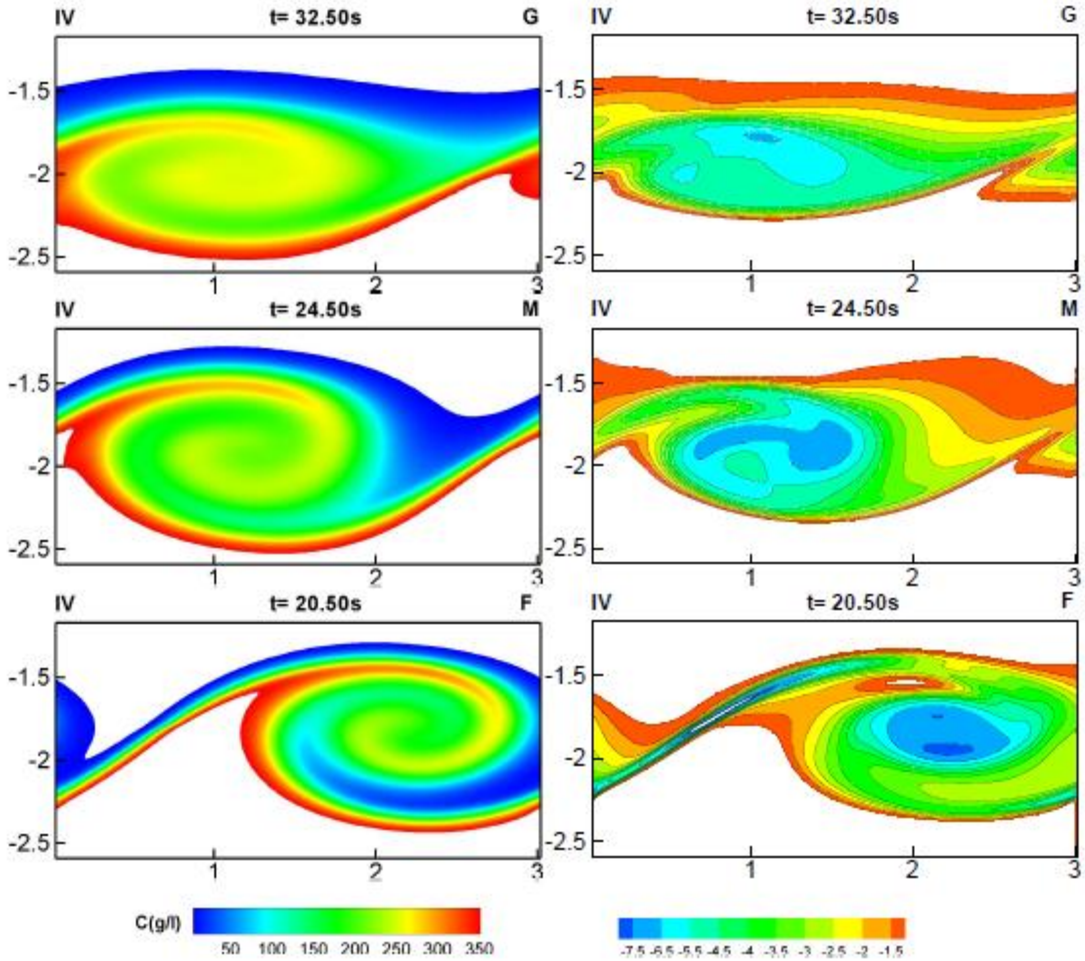

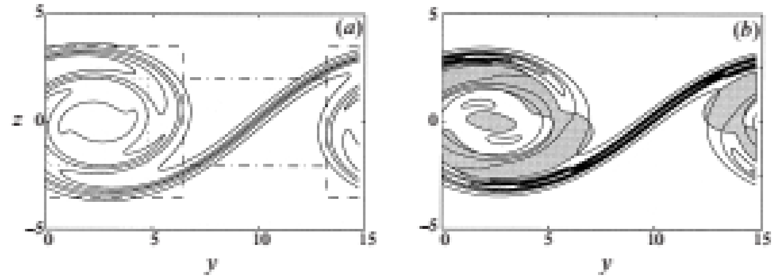

Caulfield and Peltier, JFM 2000

Compartmentalization of the flow into core (dotted rectangle), eyelid (dashed rectangle) and braid regions (dot-dashed rectangle)

Maillage	G	M	F
$t_1(s)$	25.50	20.00	17.00
$t_2(s)$	32.50	24.50	20.50
$(t_2 - t_1)(s)$	7.00	4.50	3.50
$t_{PC}(jours)$	1	3	15

Kelvin-Helmholtz Instability:
Solid and Fluid velocity and voticity differences (3/3)

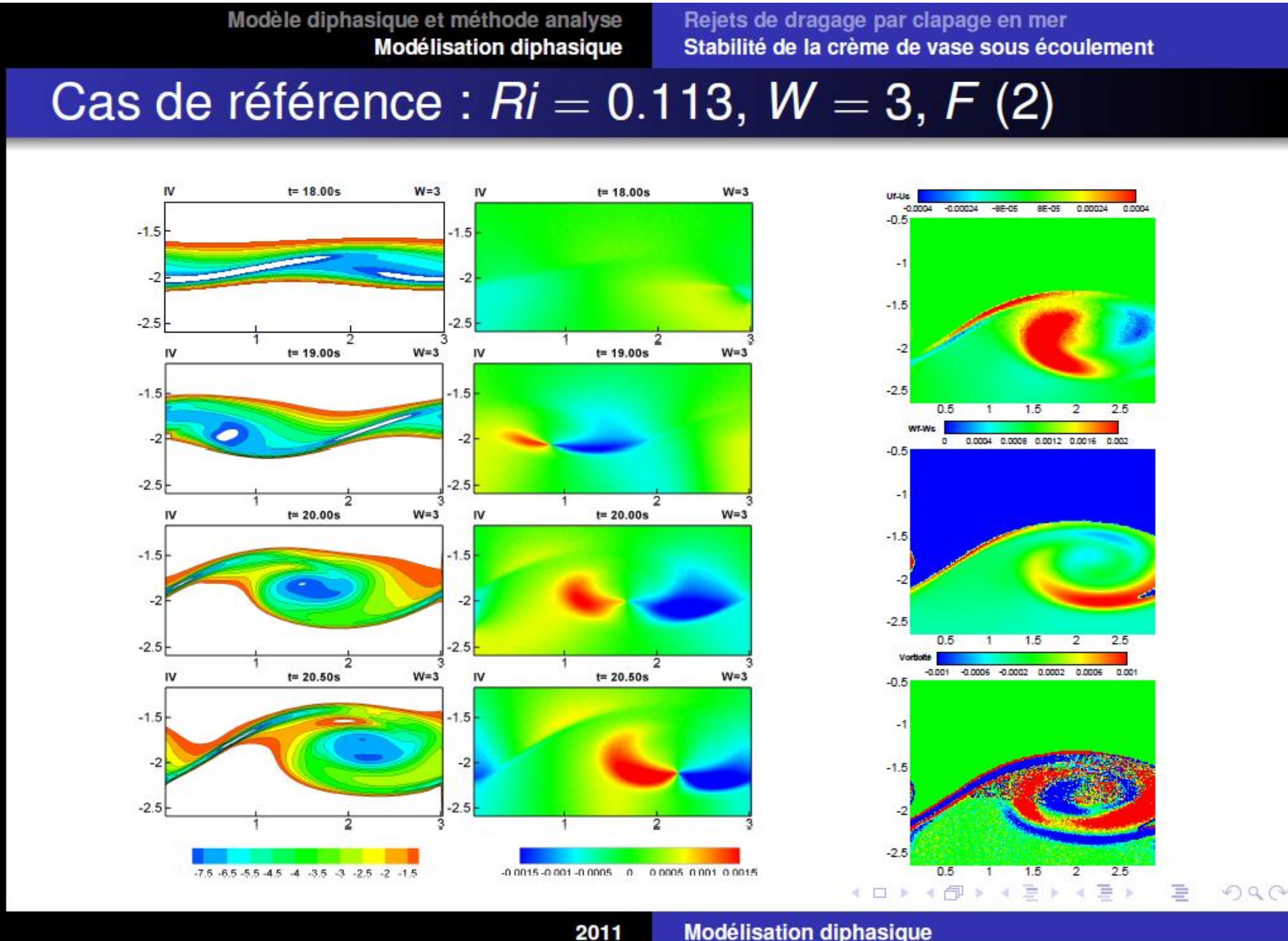

A two-phase, soil and liquid, model based on a unified formulation for continuum mechanics: application to a dredging jet

Overview

- **Part 1: Experimental investigation (Prof. P. Gondret, FAST)**
- **Part 2: Numerical modelling (NSMP, two-phase model)**

  2.1 Governing equations

  2.2 Specific Treatment for stress analysis of soil
- **Part 3: Simulation results**

  3.1 Numerical and physical parameters

  3.2 Preliminary results
- **Conclusions**

Part 1 : Experimental investigation

S. Badr, G. Gauthier, P. Gondret
THESIS'13

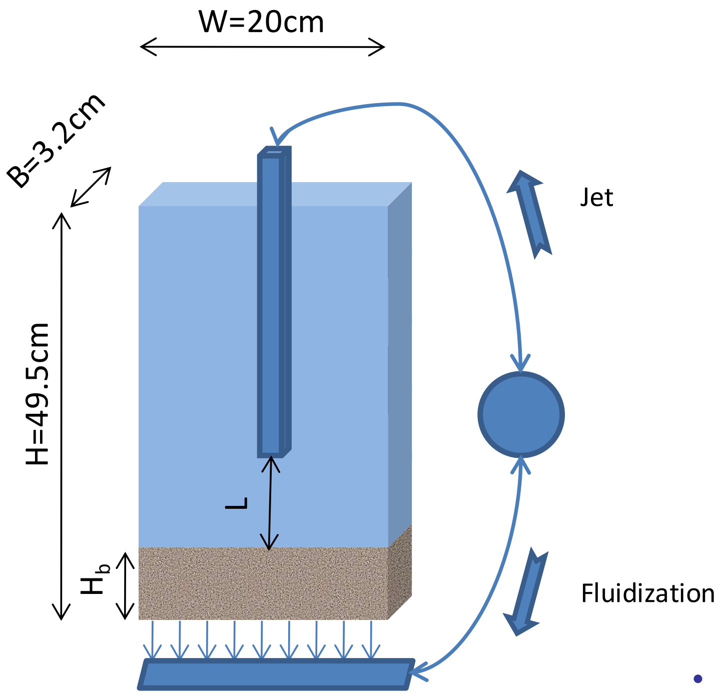

Porous flow within the granular bed

Flow conditions at the bottom boundary (previous configuration)

Craters and dunes resulting from a dynamic equilibrium

- Formation of crater by jet induced erosion
- Eroded grains create a dense suspension
- Deposition of particles at preferential locations
- Granular avalanches produced at the sandpile's surface

Geometry of craters (vertical submerged jet) as controlled by the Erosion parameter, E_c (U_0 mean velocity at the nozzle outlet; *b* dimension of the nozzle, *L* distance to the initial bed, d sediment grain size, *s* density ratio between solid and liquid). Depending on *Ec* value, the jet could be either weakly (a, b) or strongly (c,d) deflected:

redrawn from Aderibigbe & Rajaratnam [16]; figures c) and d) from Giez & Souiler [17].

a) $0.2 < E_c \leq 0.35$

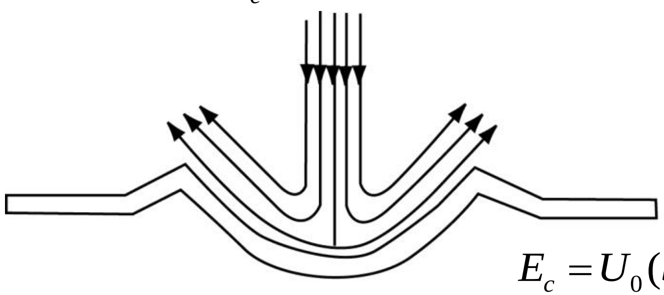

c) $0.35 < E_c \leq 2.0$

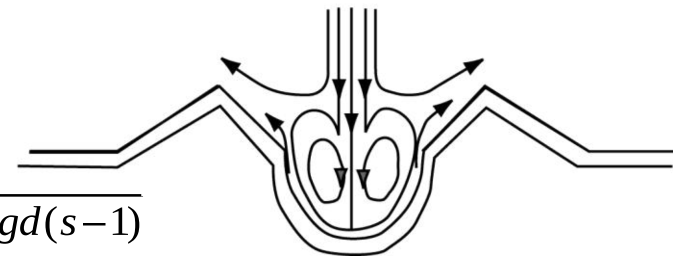

$$E_c = U_0 (b/L) \Big/ \sqrt{gd(s-1)}$$

b)

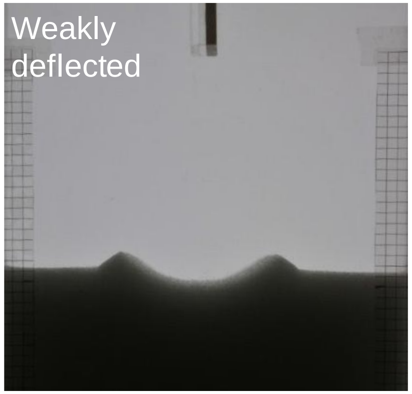

d)

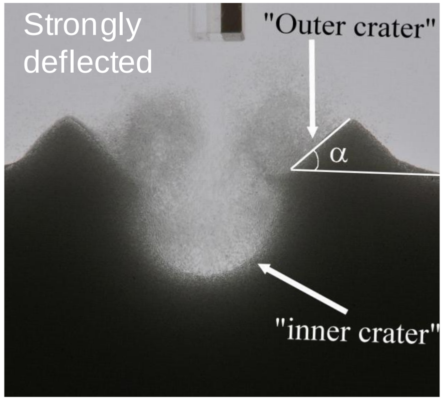

Part 2 : Numerical modelling (NSMP, two-phase model)

Two fluid pathology

S. Badr, G. Gauthier, P. Gondret
THESIS'13

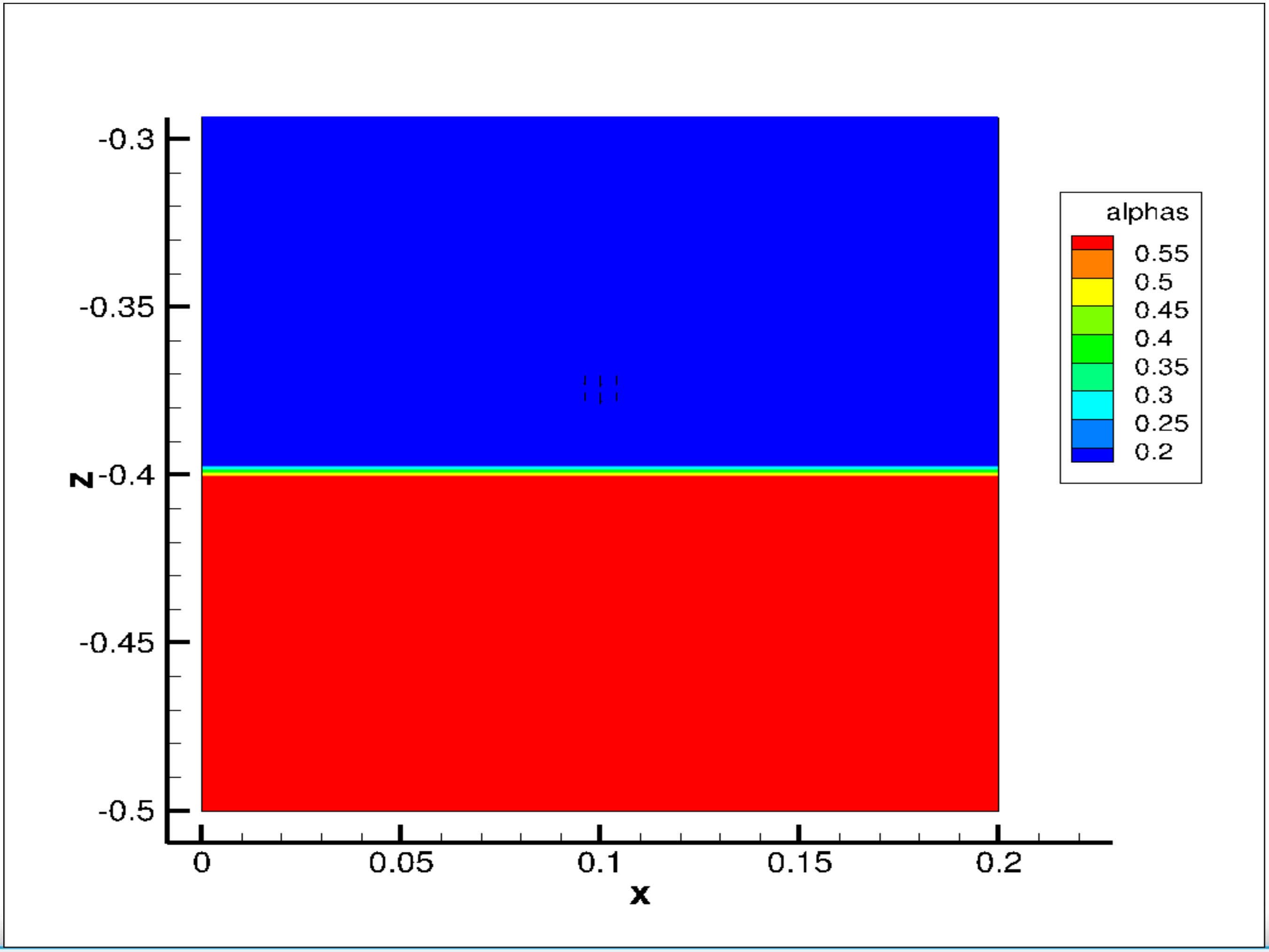

Part 2 : Numerical modelling (NSMP, two-phase model)

Governing equations [Nguyen et al (2009)]

$$\frac{D\alpha_k\rho_k}{Dt} = \frac{\partial \alpha_k\rho_k}{\partial t} + \vec{\nabla}.\left(\alpha_k\rho_k\overrightarrow{u_k}\right) = 0$$

$$\frac{D\alpha_k\rho_k\overrightarrow{u_k}}{Dt} = \vec{\nabla}.\left(\alpha_k\overline{\overline{T_k}}\right) + \alpha_k\rho_k\vec{g} + \overrightarrow{M_k}$$

Non-Newtonian, (concentration)

Momentum exchange between Phases (drag,lift, vmf)

Extension of the two-fluid approach into a fluid-soil model

Deviation in rheological behavior between granular flow and quasi-static sandpile

➔ Newtonian or Non-Newtonian Viscosity for the granular flow **(Liquid-like)**

➔ Elasticity and/or Plasticity (friction's law) for the sand heap **(Solid-like)**

Modeling strategy:

➔An unified formulation for fluid and solid phase (liquid-like and solid-like) based on continuum mechanics (no coupling)

➔The FLUID and the SOLID phase are calculated by using the FV method in the SAME computational grid

Implementation in NSMP

$$\frac{D\alpha_s\rho_s\overrightarrow{u_s}}{Dt} = \vec{\nabla}.\left(\alpha_s \overline{\overline{T_s}}\right) + \alpha_s\rho_s\vec{g} + \overrightarrow{M_s}$$

Liquid-Like

Solid-Like

Generalised Hooke's law

$$\overline{\overline{T}}_{ij}^{LL} = -p_s\overline{\overline{I}} + 2\eta(\alpha_s)\overline{\overline{\gamma}}$$

$$\overline{\overline{\gamma}} = \frac{1}{2}\left(\nabla\vec{U} + {}^t\nabla\vec{U}\right)$$

$$\eta(\alpha_s) = \mu_f\beta(\alpha_s)$$

$$U_i = \overset{\square}{D}_i$$

$$\overline{\overline{T}}_{ij}^{SL} = -p_s\overline{\overline{I}} + 2\mu\overline{\overline{\varepsilon}}$$

$$\overline{\overline{\varepsilon}} = \frac{1}{2}\left(\nabla\vec{D} + {}^t\nabla\vec{D}\right)$$

$$\lambda = \frac{\nu E}{(1+\nu)(1-2\nu)}$$

$$\mu = G = \frac{E}{2(1+\nu)}$$

For small strain

$$\overline{\overline{T}}_{ij}^{SL} = -p_s\overline{\overline{I}} + \left(2\mu\int_{t^0}^{t^n}\mathrm{dev}\left(\overset{\square}{\overline{\overline{\varepsilon}}}\right)\mathrm{dt}\right)$$

$$\square\ -p_s\overline{\overline{I}} + \left(\eta_{SL}\,\mathrm{dev}\left(\nabla\vec{U} + {}^t\nabla\vec{U}\right) + \Sigma\right)$$

$$\overline{\overline{T}}_s = (1 - f(\alpha_s)) \times \overline{\overline{T}}_s^{LL} + f(\alpha_s) \times \overline{\overline{T}}_s^{SL}$$

where

$$\eta_{SL} = \mu w_n$$

$$\Sigma = \sum_{k=0}^{n-1} w_k\,\mathrm{dev}\left(\nabla\vec{U} + {}^t\nabla\vec{U}\right)_k$$

w_k : integration coefficient

C.J. Greenshields & H.G. Weller : *Int. J. Numer. Meth. Engng* 2005; Vol. 64, pp1575-1593

Smooth transition between Liquid-Like and Solid-Like behavior

[Komatsu et al. (2001)]

solid-Like   Liquid-Like

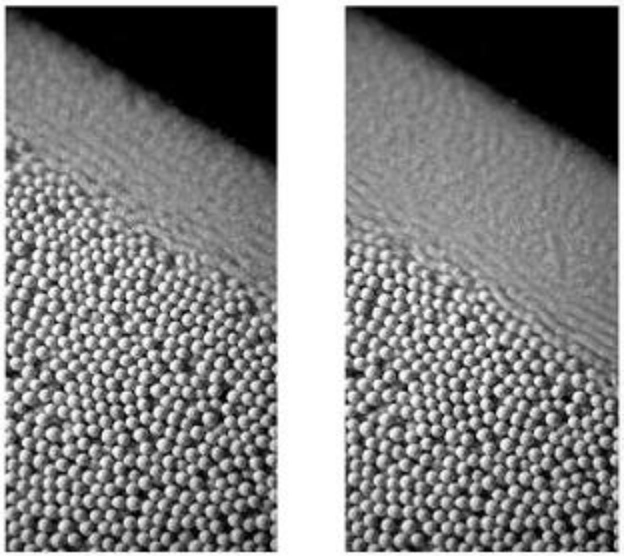

1 sec   1 min

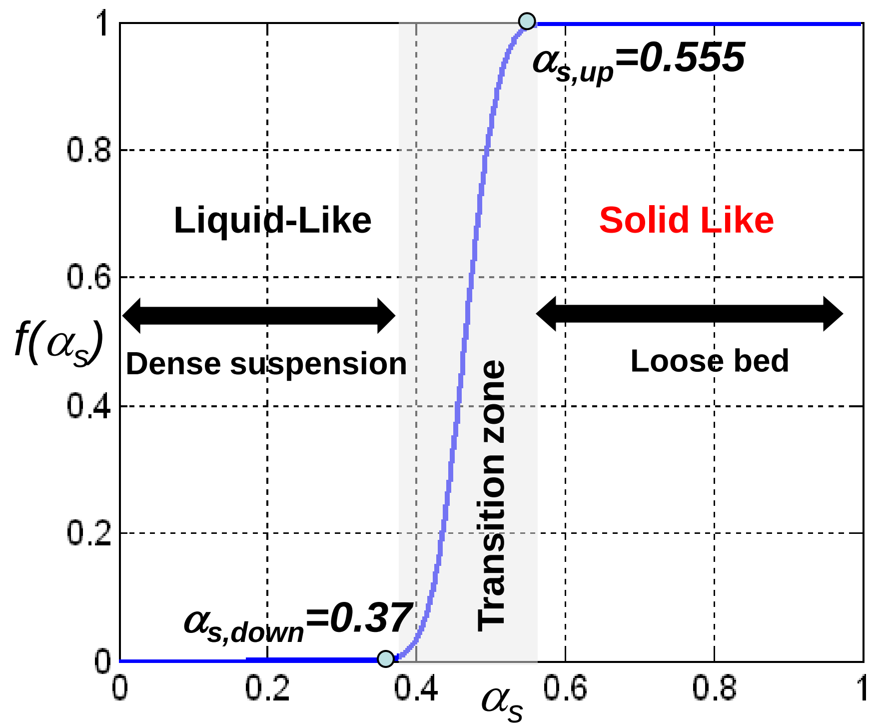

$f(\alpha_s)=f(\alpha_s,sh,sh_c)$

Sh_c – Critical Shields number

$\alpha_{s,cri}=0.465$
$\lambda=0.5$
$\delta^+=\delta^-=0.05$

Part 3 : Simulation Results

Parameters

- **Grid: 251x101** (dz=2 mm,dx=1-2 mm)
- **Initial conditions**
  - Granular bed (α_s=0.55, h=10cm)
  - Quiet water (α_s=0.0) otherwise
- **Boundary conditions**
  - impermeable : left, right of domain and jet outlet
  - Impermeable : top of the domain
  - Permeable : bottom of the domain
  - Poiseuille profile (jet outlet)
- **Time step** dt=2.10^{-5}s

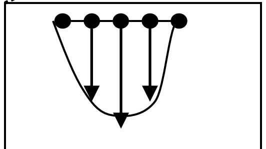
5 points
jet width: 10mm

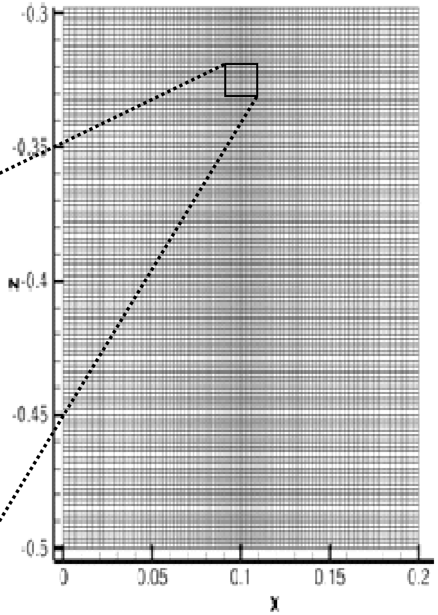

MPI version is used on IBM BlueGene P
GPU-CUDA version is under development

Elastic parameters:

Young Modulus (E) =6MPa

Poisson coefficient (ν) = 0.5

➔ Shear Modulus (G) =2MPa

➔ *'pseudo-viscosity'*

(2Gdt)=80Pa.s

➔ *'effective pseudo-viscosity'*

=80.10^{-3} m^2/s

Fluid – Soil unified model

L=2cm, Maximum velocity =0.5m/s, Average velocity =0.425m/s

Above black line F=0 and below F=1

Initial Condition at t=0.5 sec Shields Number Map

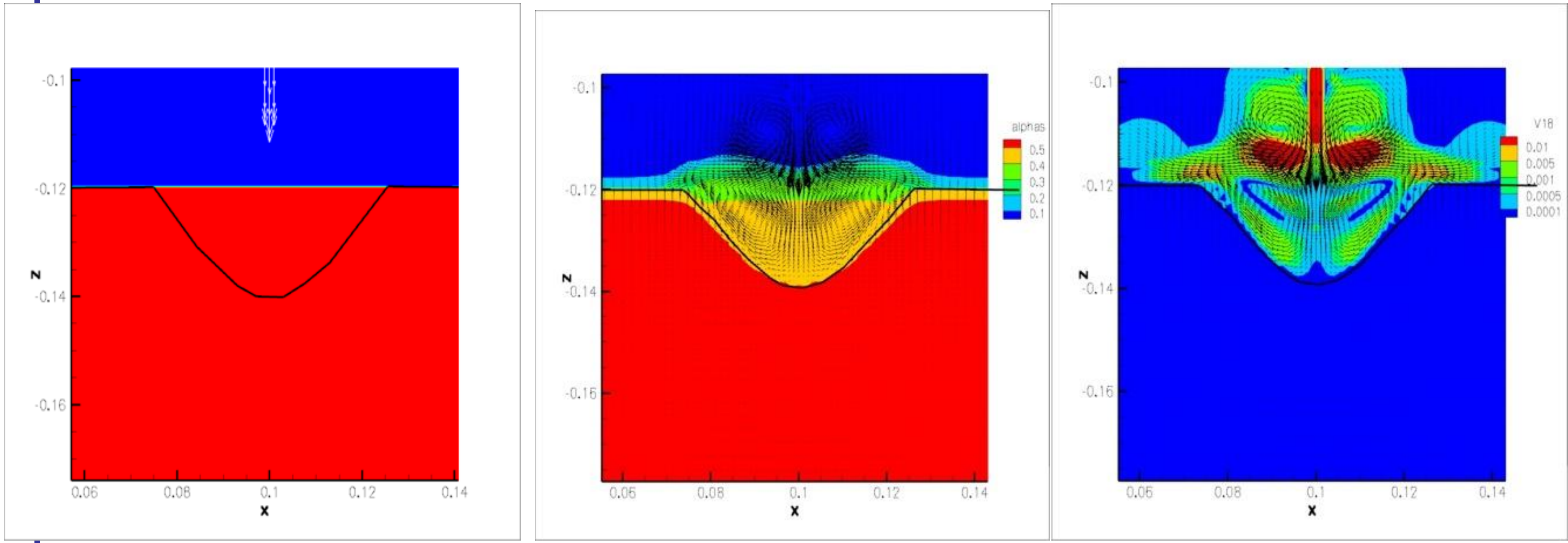

- We obtain a dynamic equilibrium of the solutuion.
- Bottom of the crater has nearly the same position than that of Shields number field .

Evolution of the crater

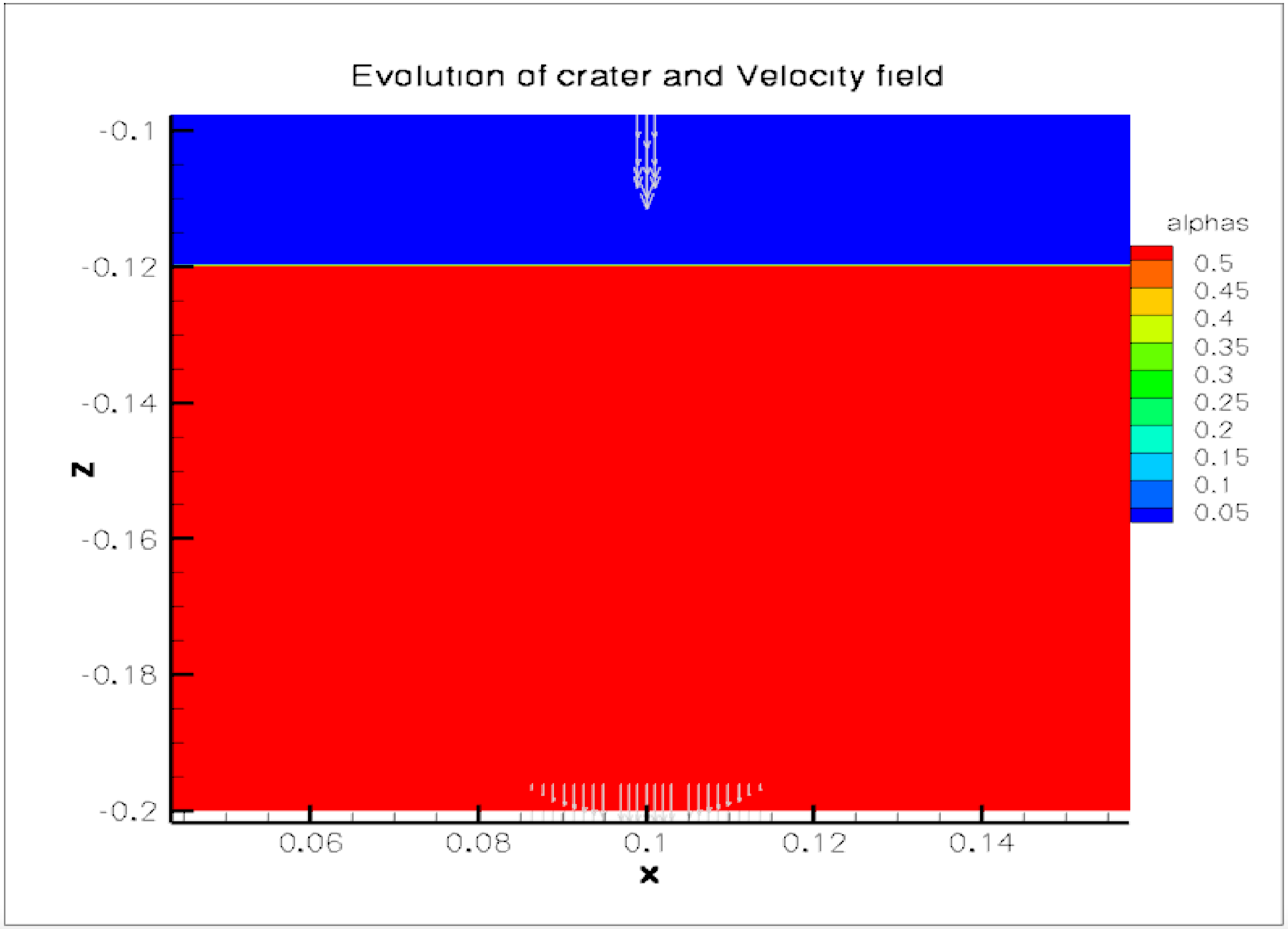

Comparison with experimental data

[Giez & Soulier (2011)]

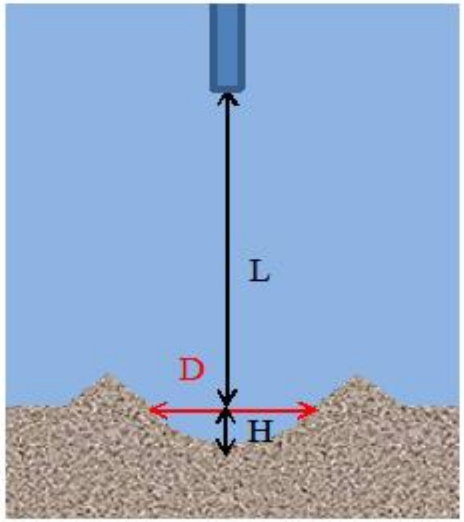

	Average velocity (m/s)	Discharge (m³/s)	Maximum velocity (m/s)	Jet Reynolds number (-)
■ (black)	0.283	2.94E-5	0.425	1133
▲ (red)	0.425	4.42E-5	0.637	1700
● (green)	0.566	5.89E-5	0.849	2267
▲ (yellow)	0.708	7.36E-5	1.062	2834
■ (blue)	0.779	8.10E-5	1.168	3117
▲ (purple)	0.850	8.84E-5	1.275	3400

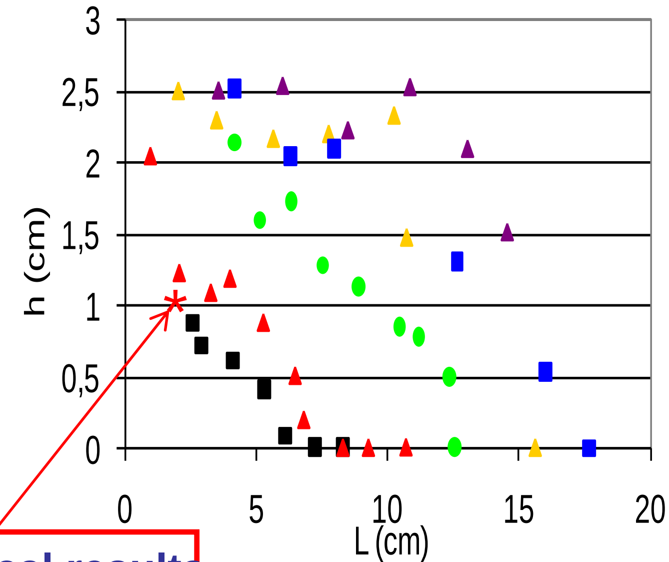

Numerical results

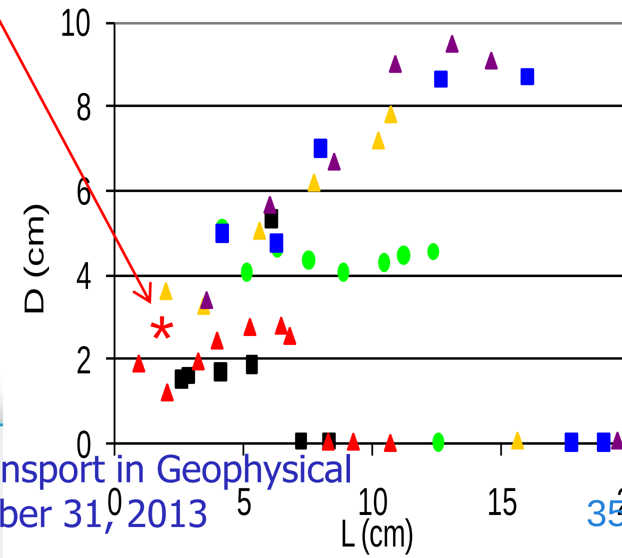

Numerical Results

Measurements

Calculations

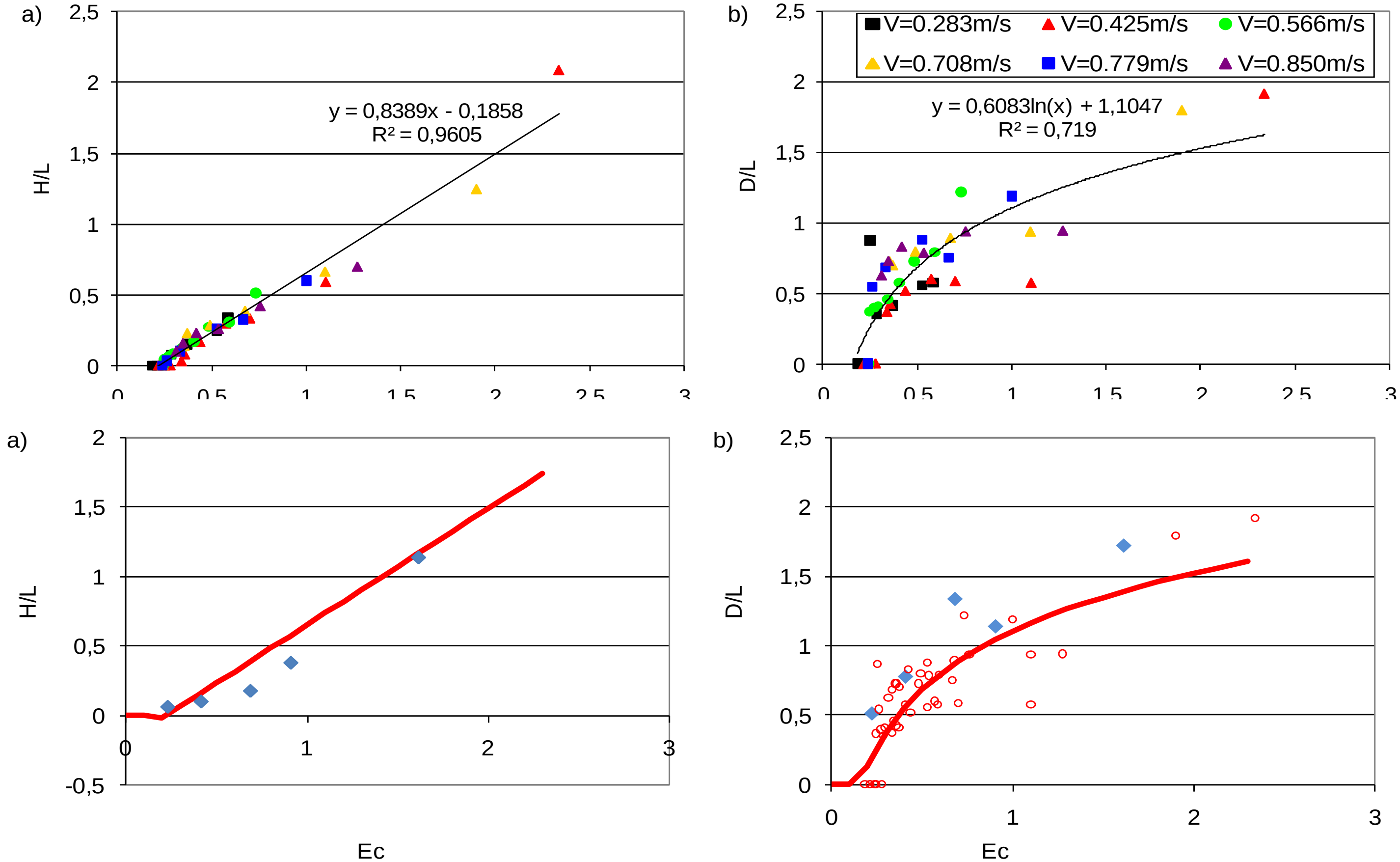

Non-dimensional characteristics of crater geometry : a) crater depth-Ec; b) crater diameter-Ec

CONCLUSIONS

- **Introduction of the proposed unified formulation gives promising results:**
  - Solid-like behaviour for solid bed is obtained.
  - Stabilised shape of the crater is obtained.
  - Quantitatively, the dimensions (H,D) of crater in good agreement with experimental observation.

- **Perspectives:**
  - More studies required on the *f*-function and its parameters.
  - Extension for other configurations (inclined, horizontal jet).
  - 3D (massively parallelized) version, application to scouring around structures, dike break.

CETMEF

APPLICATION TO THE GIRONDE ESTUARY

Coupling technique

1 confluence zone (node)/3 branches

Continuity and momentum equations integrated over the jth layer of the confluence area:

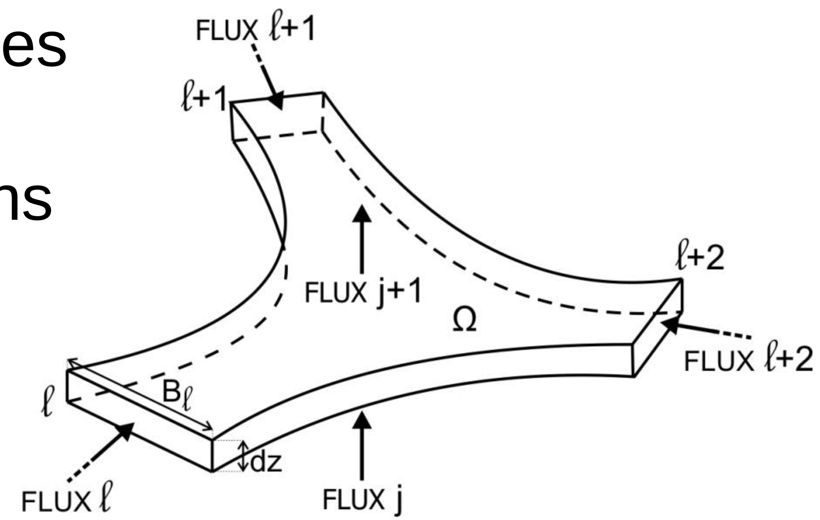

$$(\alpha_k \varphi)^{n+1} = (\alpha_k \varphi)^n - \frac{1}{\Omega} \sum_{\ell=1,3} F_\ell - \frac{1}{dz}\left(F_{j+1} - F_j\right) + S$$

Equations	Φ	Fi	Fj	S
Continuity	$\alpha_{k,no}$	$\alpha_k B_\ell u_k$	$\alpha_{k,no} w_{k,no}$	0
Momentum	$w_{k,no}$	$\frac{\alpha_k}{\rho_k}\left[p_k - \rho_k u_k w_k - \mu_{ks}\frac{\partial w_s}{\partial x} - \mu_{kf}\frac{\partial w_f}{\partial x}\right]_\ell B_\ell dt$	$\frac{\alpha_k}{\rho_k}\left[\begin{matrix} p_{k,no} + \rho_k w_{k,no} w_{k,no} - \mu_{ks}\frac{\partial w_{s,no}}{\partial z} \\ - \mu_{kf}\frac{\partial w_{f,no}}{\partial z} \end{matrix}\right]_j dt$	$\frac{1}{\rho_k} M_{kz} - \alpha_k g$

Contour map of turbidity in spring tide from the two-phase model

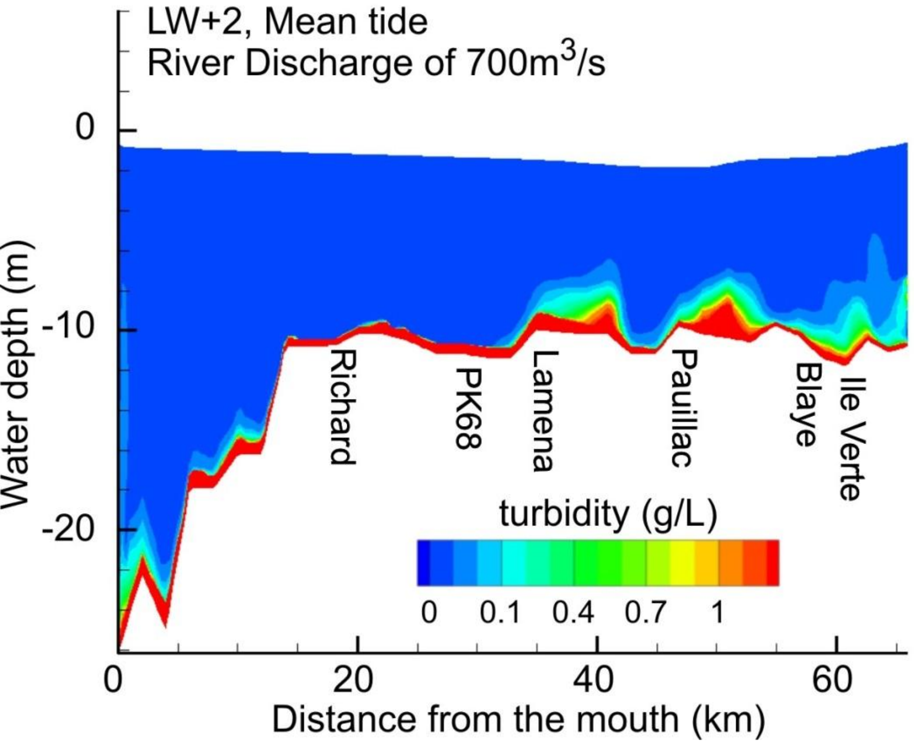

at LW+2

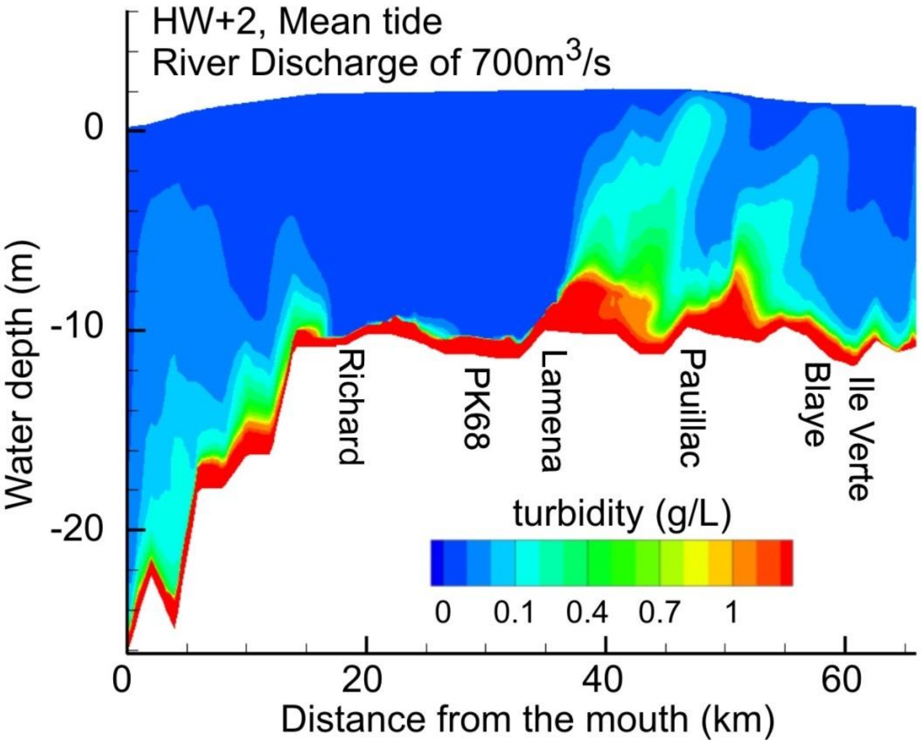

at HW+2

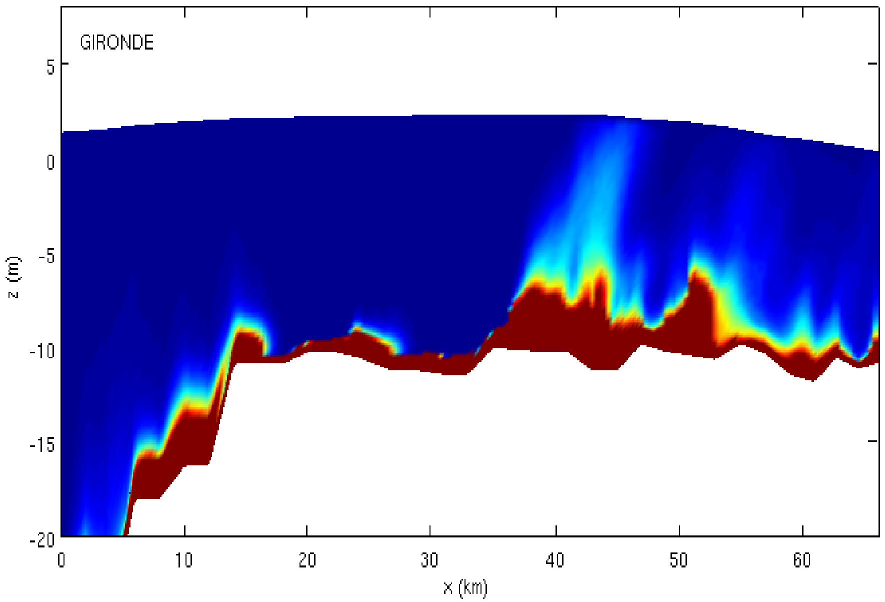
GIRONDE
z (m)
x (km)

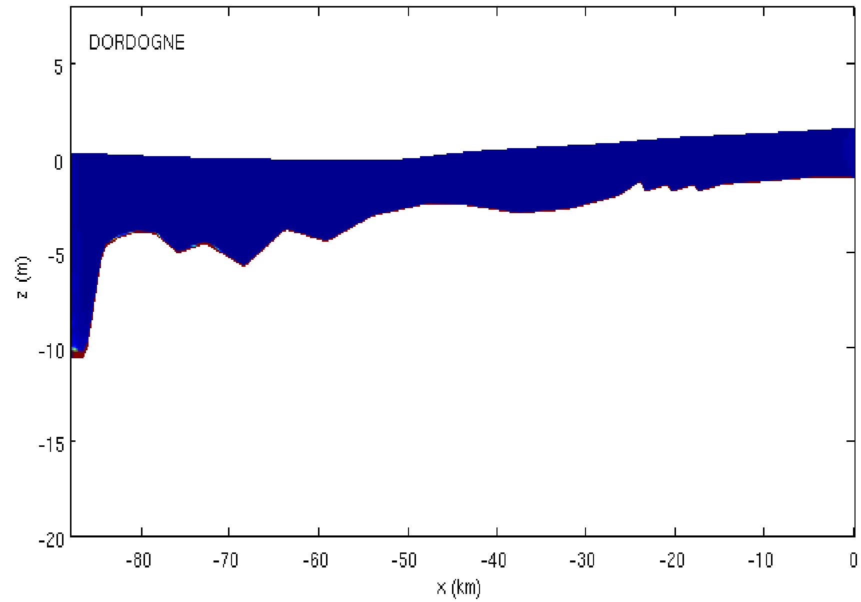
DORDOGNE
z (m)
x (km)

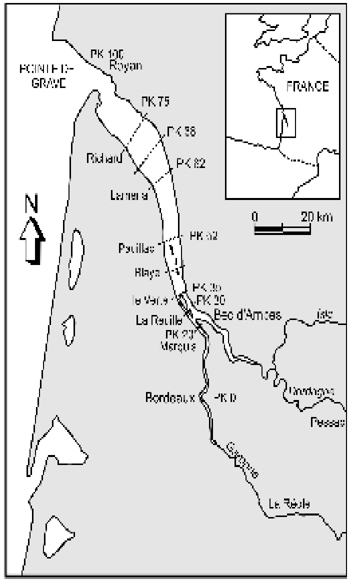
Royan
PK 75
Richard
FRANCE
0
20 km
N
Bordeaux
PK 0
Bec d'Ambes
La Réole

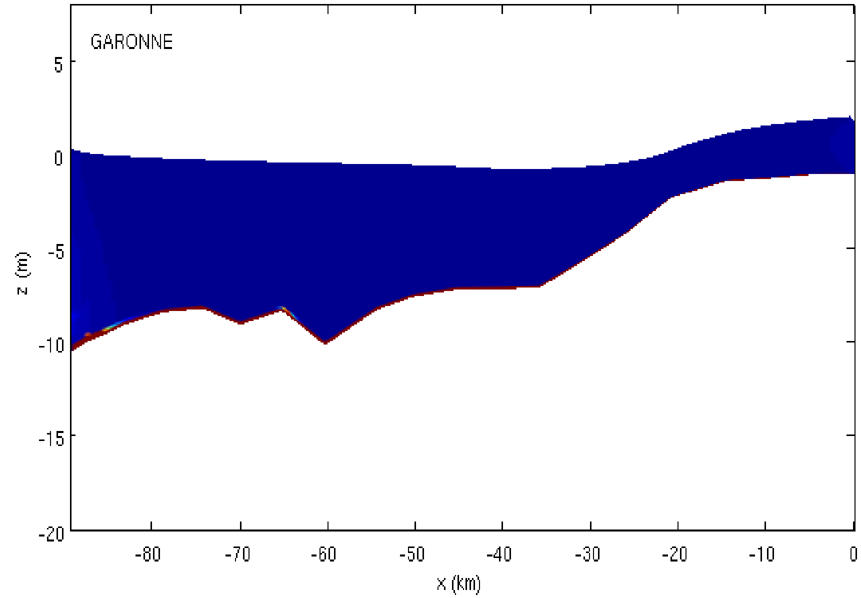
GARONNE
z (m)
x (km)

CONCLUSION

- Needing of two-phase approach
  - interactions fluid-particles, particles-particles ignored in the single phase model
  - interaction fluid-bed ⟶ only one domain
- Good behavior of the models to simulate free surface and non-hydrostatic flows and different processes of sediment transport
- New generation for modeling sediment transport ?

LABORATORY FOR HYDRAULICS

SAINT-VENANT

THANK YOU FOR YOUR ATTENTION